Adsorption of Ethyl Pyruvate on Pt(111) Studied by XPS and UPS

Thomas Bürgi,[†] Fachri Atamny,[‡] Robert Schlögl,[‡] and Alfons Baiker*,[†]

Laboratory of Technical Chemistry, ETH Zentrum, CH-8092 Zürich, Switzerland and Fritz-Haber Institut der Max-Planck Gesellschaft, Faradayweg 4-6, D-14195 Berlin, Germany

Received: January 4, 2000; In Final Form: April 18, 2000

The adsorption of ethyl pyruvate on Pt(111) at low temperature was investigated by XP and UP spectroscopy. The assignment of the photoelectron spectra was assisted by calculation of correlated ionization potentials. Comparison of the XP and UP spectra of the condensed and chemisorbed layer indicates a strong ethyl pyruvate adsorption bond in the latter. Upon chemisorption, the HOMO of ethyl pyruvate, which is a lone-pair orbital delocalized over both C═O groups, is stabilized by about 0.7 eV with respect to the other orbitals, which is characteristic for a lone-pair bonding mechanism. The same bonding mechanism was found for coverages far below saturation. The XP spectra further indicate that the ketone C═O is more strongly involved in the chemisorption bond than the carboxyl C═O of ethyl pyruvate. The packing density of the saturated chemisorbed ethyl pyruvate layer, as determined by XPS, is high. This points toward an upright or tilted orientation of ethyl pyruvate in this layer, in line with the observed bonding mechanism.

1. Introduction

Among the most complex heterogeneous catalytic systems known to date are enantioselective hydrogenations over chirally modified metal catalysts,[1] in which the interaction of an optically pure modifier with the prochiral reactant during the hydrogenation reaction determines the chirality of the product. Only two systems have been thoroughly studied to date: the Ni−tartaric acid system for the hydrogenation of β-ketoesters and 2-alkanones [2] and the Pt−cinchona system for the hydrogenation of α-ketoesters.[3] High enantiomeric excesses of 95% and more have been achieved for these systems, which, together with the inherent advantages of heterogeneous catalysts in handling and separation, makes them potentially interesting for industrial applications. Despite practical and fundamental interest in these heterogeneous enantioselective reactions, their mechanism is far from being well understood on a fundamental level.

For the Pt−cinchona system, the enantioselective hydrogenation of ethyl pyruvate (EP, Scheme 1) has been used as a model in many studies. Among the many mutual interactions between modifier, ethyl pyruvate, hydrogen, Pt catalyst, and solvent, which are important for the functioning of this complex catalytic system, the interaction between the Pt surface and ethyl pyruvate has not yet been explicitly addressed. Specifically, open questions with significant importance for the understanding of the catalytic reaction are the interaction mechanism involved in the bonding of ethyl pyruvate to the Pt surface, i.e., which orbitals are involved in the bonding and whether ethyl pyruvate adsorbs in a parallel or perpendicular mode. In the proposed mechanistic models, the ethyl pyruvate is thought to adsorb on the Pt surface in a parallel π-bonding mode.[4−6]

The bonding mechanism involved in the interaction of α-ketoesters with transition metal surfaces has not yet been studied. The bonding is likely to be dominated by the two C═O groups. Two adsorption modes can be anticipated, in analogy with aldehydes and ketones.[7−9] In the first, the bonding is dominated by the oxygen lone pairs. In this mode, the C═O groups have a tendency to be oriented in an upright position (perpendicular mode). In the second mode, the π system of the C═O groups is involved in the bonding, with the C═O group lying parallel to the surface (parallel mode). For acetone, for example, both modes have been observed experimentally. On Pt(111), the perpendicular mode dominates,[10] in agreement with theoretical work.[8] On clean Ru(001), on the other hand, the parallel mode prevails.[10,11]

In the following, we present XPS and UPS investigations on the adsorption of ethyl pyruvate on Pt(111) at low temperatures, which provide new insight into the interaction mechanism. In section 2, the experimental details are given. The results are presented in section 3 and discussed in section 4. Conclusions will be drawn in section 5.

2. Experimental Section

Experiments. The X-ray and the ultraviolet electron spectroscopy (XPS and UPS), as well as the thermal desorption spectroscopy (TDS) measurements, were carried out in an UHV apparatus consisting of four chambers (XPS/UPS, TDS, high-pressure chamber (reactor), and load-lock) built around an UHV transfer chamber. The sample was mounted on a transferable sample holder, where it could be heated to 1400 K by electron impact and cooled to 130 K by a liquid nitrogen cooling system in both the XPS/UPS and TDS chambers.

The XPS and UPS measurements were performed on a Leybold Heraeus LHS11 MCD instrument upgraded with a multichannel detector. Mg Kα radiation (240 W) was used to excite photoelectrons, which were detected by the analyzer operated at 31.5 eV constant pass energy. The photon energies used for UPS and XPS were 21.21 eV (He I) (2.52 eV pass energy), 40.82 eV (He II) (12 eV pass energy), and 1254.6 eV (Mg Kα), respectively. The instrumental resolution was 0.13 eV in the UPS (He I) mode, as estimated from the Fermi edge cutoff, and 0.95 eV in the XPS mode, as determined by the full

* Author to whom correspondence should be addressed. Fax: ++41 1 632 11 63. E-mail: baiker@tech.chem.ethz.ch.
[†] ETH Zentrum.
[‡] Fritz-Haber Institut der Max-Planck Gesellschaft.

10.1021/jp0000127 CCC: $19.00 © 2000 American Chemical Society
Published on Web 06/02/2000

width at half-maximum of the Au $4f_{7/2}$ line at 84.2 eV. The energy scale of the spectrometer was calibrated versus the Au $4f_{7/2}$ line at 84.2 eV, the Ag $3d_{5/2}$ line at 367.9 eV, and the Cu $2p_{3/2}$ line at 932.4 eV. The work function was determined from the total width of the UP spectra. The base pressure in the TDS chamber was below 2×10^{-10} mbar, and in the XPS/UPS chamber, below 8×10^{-11} mbar. Temperature was measured with a chromel−alumel thermocouple spot-welded to the side of the crystal.

The Pt(111) single crystal was cleaned by repeated Ar^+ bombardment (3.5 kV, 5×10^{-6} mbar of Ar) and subsequent annealing at 1400 K. The cleanness of the crystal was checked using both XPS and UPS experiments, in which no impurities were detected and a characteristic UP spectrum of Pt(111) was measured.

TDS experiments were carried out at a linear heating rate of 2 K/s. Desorption signals from the sample-holder system were monitored in blank runs. All TDS measurements were performed using a quadrupole mass spectrometer (QMS) with the ionizer in line-of-sight to the sample surface. To reduce contributions from background (crystal back, edges, surrounding, etc.) the QMS was equipped with a shield cup with a small opening aperture. The crystal was positioned 2 mm from the entrance aperture of the QMS shield.

During exposure and measurement, the Pt(111) crystal was held at a temperature of 150 K, if not otherwise indicated. Ethyl pyruvate (Aldrich, 98%) was purified by repeated freeze−pump−thaw cycles. Ethyl pyruvate was dosed with a needle doser. During dosing, the background pressure in the chamber was around 1×10^{-9} mbar.

Coverage was determined via the O1s/Pt4f signal ratio from the XPS spectra. A saturated chemisorbed layer was prepared by dosing ethyl pyruvate onto the Pt(111) sample at 150 K followed by heating to 213 K, thus desorbing the physisorbed (multilayer) ethyl pyruvate. The O1s/Pt4f signal ratio of this surface was defined as one monolayer (ML). Fractional coverages were determined by comparing the O1s/Pt4f signal ratio with the ratio at 1 ML.

Absolute coverage was determined via XPS with a saturated CO layer serving as the calibration standard. This layer was prepared by exposing the clean Pt(111) sample to 600 L (1L = 10^{-6} Torr s) of CO while cooling it from room temperature to 153 K. Such a layer showed two separate signals in the O1s region, at 531.0 and 532.7 eV, corresponding to CO in bridge and on-top sites, respectively.[12] The ratio of the integrated intensity of the two signals was 1:2, as expected for a saturated CO layer on Pt(111). The coverage of this layer is $\Theta_{CO} = 0.6$ ML, i.e., 0.6 O atoms per Pt surface atom.[12] The absolute coverage of ethyl pyruvate, Θ_{EP}, was determined from the integrated O1s/Pt4f signal ratio R_{EP} by using the integrated O1s/Pt4f signal ratio for the saturated CO layer R_{CO} as $\Theta_{EP} = {}^1/_3\, R_{EP}/R_{CO}$ 0.6 ML, thus neglecting signal attenuation from diffraction or shielding. The factor of $^1/_3$ in the above equation arises because EP has three O atoms.

Calculations. To help with the assignment of the XP and UP spectra, electronic structure calculations were performed using the Gaussian 94 suite of programs.[13] Semiempirical PM3 calculations[14] were used to obtain a qualitative picture of the molecular orbitals of ethyl pyruvate. The outer valence Green's function (OVGF) method[15] was used with a 6-31G(d,p) standard basis set to calculate correlated ionization potentials (IPs). Prior to the OVGF calculations, the structure of ethyl pyruvate was fully optimized at the Hartree−Fock level.

SCHEME 1: Ethyl Pyruvate

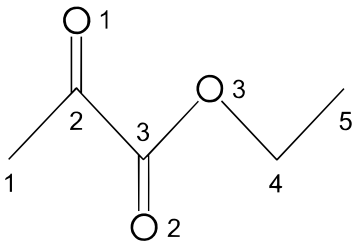

TABLE 1: Calculated Binding Energies (eV) with Respect to the Vacuum Level for C and O 1s Electrons of Ethyl Pyruvate[a]

	HF		OVGF	
atom	absolute	relative	absolute	relative
C3	310.0/309.9	0.0/0.0	298.0/298.0	0.0/0.0
C2	308.9/308.8	1.1/1.1	297.1/297.1	0.9/0.9
C4	307.4/307.5	2.6/2.4	296.0/296.1	2.0/1.9
C1	305.8/305.9	4.2/4.0	294.2/294.3	3.8/3.7
C5	305.5/305.7	4.5/4.2	294.2/294.4	3.8/3.6
O3	561.1/561.1	0.0/0.0	547.2/547.3	0.0/0.0
O1	560.1/560.1	1.0/1.0	546.6/546.6	0.6/0.7
O2	559.8/559.7	1.3/1.4	546.2/546.2	1.0/1.1

[a] HF orbital energies as well as correlated ionization potentials calculated using the OVGF method are given. Calculations were performed using a 6-31G(d,p) basis set. Relative values are with respect to the most stable C and O 1s electrons. The first binding energy corresponds to the s-trans, the second to the s-cis, conformer. Atom numbering is according to Scheme 1.

3. Results

3.1. Molecular Orbitals. Ethyl pyruvate (EP, Scheme 1) exists in two conformers s-cis and s-trans, which differ by the dihedral angle O=C−C=O (0° for s-cis and 180° for s-trans). Conformer s-trans, which is depicted in Scheme 1, is more stable in the gas phase by 1−2 kcal/mol,[16] but the relative stability could be strongly influenced by the metal surface, especially because the s-cis conformer has a considerably larger dipole moment.[16] Hence, we have performed all of the calculations for both s-cis and s-trans EP.

Calculated binding energies of the C and O 1s electrons of EP are reported in Table 1. Atom numbering is according to Scheme 1. The binding energies were calculated at both the Hartree−Fock (HF) and the outer valence Green's function (OVGF) levels and are given with respect to the vacuum niveau. A comparison of the values in Table 1 with the ones measured for gas-phase ethyl propionate[17] shows that the binding energies (BEs) calculated at the OVGF level are overestimated by about 4 eV (1.4%) for C 1s and 8 eV (1.5%) for O 1s, whereas at the HF level, the BEs are too high by about 15 and 22 eV (5.2 and 4.2%), respectively. Despite this discrepancy in absolute BE values, the calculated BE *differences* for the different C and O 1s electrons (also reported in Table 1) should provide valuable estimates and will be compared with those derived from the XP spectra of EP. It can be seen from Table 1 that the 1s electron of C3 is the most strongly bound, followed by C2, and C4. The 1s BEs of the three O atoms are within about 1 eV of each other. It is also clear from Table 1 that the conformation of EP (s-cis vs s-trans) has only a marginal effect on the 1s BEs.

The molecular orbital approach has been successfully applied to achieve a qualitative understanding of the bonding mechanism for adsorbates on metal surfaces. To get an overview of the frontier orbitals of EP, which are involved in the bonding to the Pt(111) surface, we have performed PM3 molecular orbital

TABLE 2: Calculated Ionization Potentials (eV) with Respect to the Vacuum Level for Orbitals near the HOMO−LUMO Gap of Ethyl Pyruvate[a]

			energy (eV)		
orbital	label	symmetry	PM3	HF	OVGF
LUMO+2	π^*_2	a″	1.4/1.4		
LUMO+1		a′	0.9/1.0		
LUMO	π^*_1	a″	−0.4/−0.3		
HOMO	$n_{0(O1,O2)}$	a′	−10.9/−10.9	−11.3/−11.5	−9.5/−9.7
HOMO−1	$n_{0(O3)}$	a″	−11.5/−11.6	−12.7/−12.7	−11.4/−11.4
HOMO−2	$n_{0'(O1,O2)}$	a′	−12.5/−12.4	−13.8/−13.2	−11.9/−11.4
HOMO−3	$\sigma_{C-C,C-O}$	a′	−13.1/−13.2	−14.2/−14.4	−12.8/−13.0
HOMO−4	$\pi_{C=O}$	a″	−12.8/−12.9	−13.9/−13.9	−13.0/−13.0
HOMO−5	$\pi_{C=O}$	a″	−13.4/−13.4	−14.3/−14.5	−13.3/−13.5

[a] PM3, HF, and OVGF values are given. For HF and OVGF, a 6-31G(d,p) basis set was used. Symmetry labels are for C_s symmetry. First energy for s-trans, second energy for s-cis, conformer.

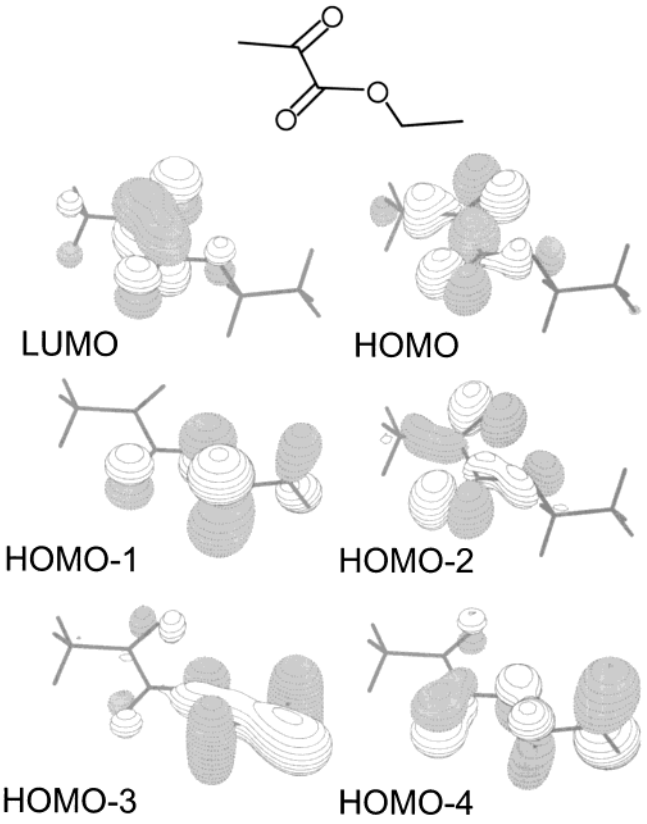

Figure 1. Pictorial representation of some molecular orbitals of ethyl pyruvate. The orbitals were calculated at the semiempirical PM3 level.

calculations. Figure 1 depicts the six orbitals, from the LUMO to the HOMO-4, for s-trans EP, and Table 2 lists the corresponding ionization energies. As compared to CO, for example, EP is a relatively large molecule with delocalized molecular orbitals. The LUMO is a π^* orbital, which is delocalized over both carbonyl groups. The three highest-occupied orbitals (HOMO through HOMO-2) can be best described as lone-pair orbitals. HOMO and HOMO-2 have a' symmetry and can be viewed as symmetric and antisymmetric combinations of the lone pairs at O1 and O2 [$n_{O(O1,O2)}$, $n_{O'(O1,O2)}$]. HOMO-1 is the lone pair at O3 and is of a'' symmetry [$n_{O(O3)}$]. HOMO-3 is a $\sigma_{C-C,C-O}$ orbital, and HOMO-4 can be viewed as a $\pi_{C=O}$ orbital with a considerable contribution at the C5 methyl group. The molecular orbital coefficients are very similar for s-cis and s-trans EP, and the molecular orbitals for s-cis EP (not shown) are very similar to those for s-trans EP.

The orbital (ionization) energies were calculated at the PM3, HF, and OVGF levels and reported in Table 2. The OVGF results are expected to be the most accurate and will be compared with the UPS measurements below. The OVGF calculations predict the HOMO to be less stable by almost 2 eV than HOMO-1 and HOMO-2, which are close in energy. Between HOMO-2 and HOMO-3, there is again a gap of about 1 eV. According to the HF and OVGF calculations, the energy of the HOMO and HOMO-2 lone-pair orbitals is influenced by the conformation of EP. The HOMO is slightly stabilized when going from s-trans to s-cis, whereas HOMO-2 is destabilized. This can be understood on the basis of the molecular orbitals depicted in Figure 1. In the s-cis conformation, the lone pairs at O1 and O2 are interacting with each other because of close proximity. For the HOMO, this interaction is bonding, leading to stabilization, whereas for HOMO-2, it is antibonding, leading to destabilization.

3.2. XPS. To discriminate between conditions under which monolayer and multilayer adsorption occurred, thermal desorption spectroscopy (TDS) was applied. The TD spectra showed that desorption of the physisorbed multilayer occurred at 208 K, in agreement with the XPS measurements. Figure 2 shows the C1s XPS spectra of ethyl pyruvate measured at 153 K (a) in the condensed phase (about 10 ML) and (b) at monolayer coverage. Also shown are fits to a mixture of Gaussian and Lorentzian functions. The results of the fits are reported in Table 3. Figure 3 shows the analogous O1s spectra. The C1s spectrum of the condensed phase is characterized by peaks at 290.6 and 287.1 eV and a shoulder at 288.4 eV. The integrated intensity of the peak at 290.6 eV amounts to 40% of the total intensity of the C1s spectrum and corresponds to two C atoms. The spectrum could be well fit with four bands (Gaussian−Lorentzian functions), as shown in Figure 2. The three bands at 291.2, 290.3, and 288.7 eV have about equal intensity and correspond to C3, C2, and C4 (see Scheme 1 for numbering), whereas the band at 287.1 eV is twice as intense and corresponds to C1 and C5, which have very similar binding energies. The carboxyl C3 has the highest C1s binding energy, followed by the ketone C2. C1 and C5 have the lowest binding energies. The relative 1s binding energies with respect to C3, as given in Table 3, agree well with the calculated values given in Table 1, confirming the above assignments. The full width at half-maximum (fwhm) of the individual bands is about 1.7 eV, as can be seen from Table 3.

When going from multilayer to monolayer coverage (Figure 2), the whole spectrum is shifted by about 3 eV to lower binding energies. Two peaks at 288.1 and 284.8 eV can be observed. The spectrum also exhibits a marked change in shape. Compared to the feature in the multilayer spectrum, the high-energy peak is less intense, corresponding to only C3. The spectrum was again fit with four bands. The assignments, together with the

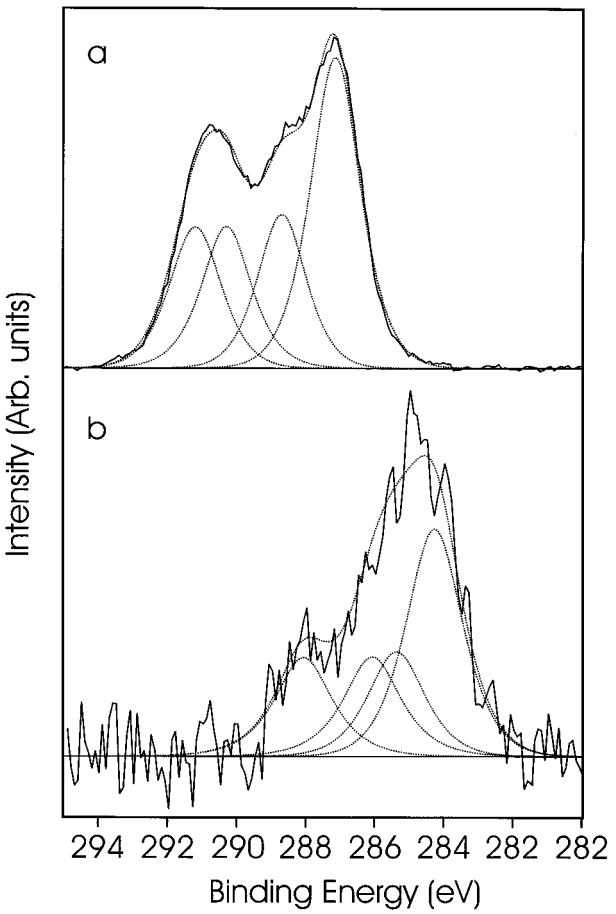

Figure 2. C1s XP spectrum of ethyl pyruvate on Pt(111) at 153 K. (a) Condensed phase. (b) Monolayer. Dashed lines correspond to a fit of Gauss−Lorentz functions to the measured spectra.

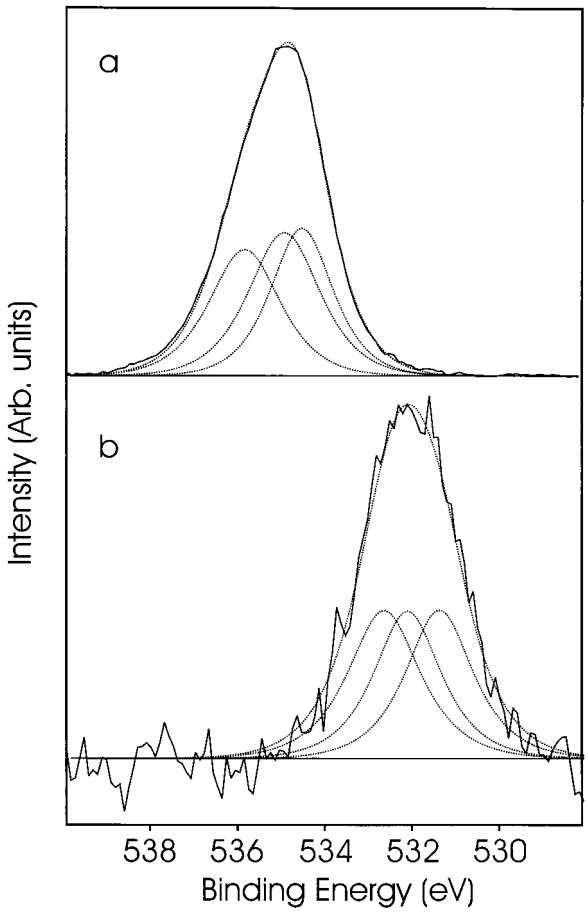

Figure 3. O1s XP spectrum of ethyl pyruvate on Pt(111) at 153 K. (a) Condensed phase. (b) Monolayer. Dashed lines correspond to a fit of Gauss−Lorentz functions to the measured spectra.

TABLE 3: C1s and O1s Binding Energies (BE, eV) of Ethyl Pyruvate in the Condensed Phase and One Monolayer Adsorbed on Pt(111)

	multilayer				monolayer			
atom	abs BE	rel BE	fwhm	Lorentz	abs BE	rel BE	fwhm	Lorentz
C3	291.2	0.0	1.8	60	288.1	0.0	2.0	80
C2	290.3	0.9	1.7	72	286.1	2.0	2.0	80
C4	288.7	2.5	1.7	61	285.4	2.7	2.0	68
C1, C5	287.1	4.1	1.8	67	284.3	3.8	2.0	66
O3	535.9	0.0	1.9	69	532.7	0.0	2.0	80
O1	535.0	0.9	2.0	69	532.2	0.5	1.9	80
O2	534.6	1.3	1.7	71	531.5	1.2	1.9	80

[a] Energies were obtained by fitting a mixture of Gaussian and Lorentzian functions to the experimental spectra displayed in Figures 2 and 3. Also given are the full width at half-maximum (fwhm) and the contribution (%) of the Lorentzian function. Atom labeling is according to Scheme 1. Relative values are with respect to the largest binding energy.

obtained binding energies, are reported in Table 3. The results indicate that C2 (ketone group) exhibits a prominent shift in C1s binding energy with respect to the other C atoms of ethyl pyruvate, when going from multi- to monolayer. Also, the fwhm of the bands is increased (Table 3).

The O1s spectrum of the multilayer shown in Figure 3a consists of one peak centered at 534.8 eV, which is slightly asymmetric toward the high-energy side. This asymmetry is caused by the unequal spacing between the bands corresponding to O1, O2, and O3, as shown by the fit in Figure 3 and Table 3 and as predicted by the calculations (Table 1). The highest O1s binding energy is associated with O3, followed by O1. Upon going to the monolayer, the O1s spectrum shifts by about 3 eV to lower binding energy, analogously to the C1s spectrum. The peak centered at 532.2 eV for the monolayer seems to be more symmetric than that for the multilayer, indicating more equal spacing between the individual bands, as given by the fit.

After desorption of the multilayers, the absolute EP coverage was $\Theta_{EP} = 0.23 \pm 0.045$ ML (95% confidence interval), as determined by XPS using the procedure described in the Experimental Section. Thus, one EP molecule occupies four to five surface Pt atoms in the saturated chemisorbed layer.

3.3. UPS. *Assignment of Multilayer Spectrum.* The UP spectrum of a multilayer of EP adsorbed on Pt(111) can be assigned using the results of the OVGF calculations presented in Table 2. This procedure involves the assumption that the (calculated) gas-phase spectrum is similar to the (measured) spectrum of physisorbed EP in the multilayer, which proved to be a good assumption for other molecules.[18] Figure 4 shows the He(II) UP spectrum, and Figure 5 (trace 1) the He(I) UP spectrum, of 2.6 ML of EP, which was dosed onto the Pt(111) crystal at 153 K. The spectra were recorded at the same temperature. In Figure 4, the calculated ionization potentials with respect to the Fermi level are also shown. Black bars correspond to ionization from orbitals with a' symmetry, and white bars from orbitals with a'' symmetry. Also shown in Figure 4 are the calculated pole strengths, which are a measure of the ease of the ionization. The band nearest to the Fermi level in the multilayer spectrum appears at about 4.1 eV. This band can unambiguously be assigned to the lone-pair orbital

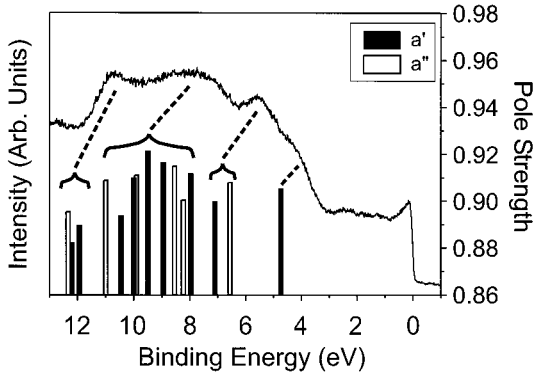

Figure 4. UP spectrum (He II) of ethyl pyruvate multilayer adsorbed on Pt(111) and calculated correlated ionization potentials (IPs) as determined by the outer valence Green's function (OVGF) method using a 6-31G(d,p) basis set. The right ordinate gives the calculated pole strength, which is a measure of the ease of the ionization. The calculated IPs are referred to the Fermi level by subtracting the work function from the IP as calculated with respect to the vacuum level. Black and white bars correspond to ionization from orbitals with a' and a'' symmetry, respectively (within C_s).

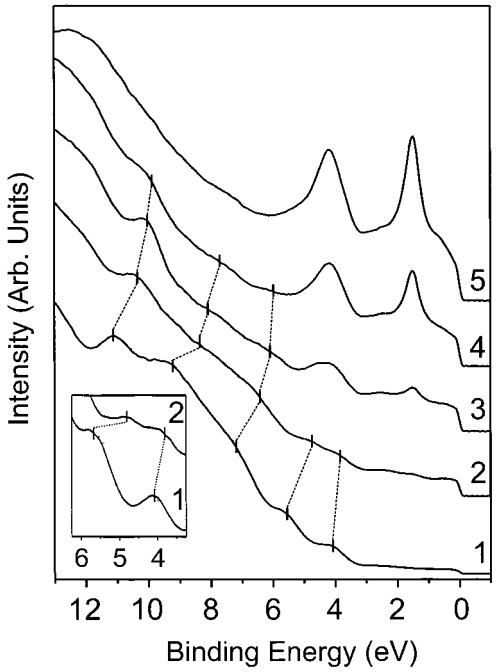

Figure 5. UP spectra (He I) of ethyl pyruvate adsorbed at 153 K onto clean Pt(111). The coverages, as determined by XPS, are (1) 2.6 ML (multilayers), (2) 1.2 ML, (3) 0.7 ML, and (4) 0.4 ML. The spectrum of clean Pt(111) is also given (5).

n_0(O1, O2). The calculations (Table 2) give an ionization potential of 9.5 eV with respect to the vacuum level. This corresponds to a value of 4.7 eV with respect to the Fermi level, taking the work function into account, in reasonable agreement with the experiment. The next band in the multilayer spectrum appears at a 1.5-eV higher binding energy. This band is assigned to the lone-pair orbitals n_0(O3) and n_0'(O1, O2). The OVGF calculations predict an energy gap between n_0(O1, O2) and n_0-(O3) of 1.9 eV. According to the OVGF calculations, there is a gap of about 1 eV to the next orbitals, which are a $\sigma_{C-C,C-O}$ and the two $\pi_{C=O}$ orbitals. Starting with these orbitals, the calculated density of orbitals is quite high up to 11 eV. This is in good agreement with the He(II) and He(I) UP spectra in Figures 4 and 5, which exhibit a broad band ranging from about 7 to 10 eV. After a narrow gap, a prominent band is again observed at 10.8 eV, which is associated with the π_{C-H} and σ orbitals. In summary, the binding energies calculated at the OVGF level and corrected for the work function are about 1 eV too high. However, the energy spacing between the orbitals is very well reproduced, as demonstrated in Figure 4.

Coverage Dependence. Figure 5 shows the UP spectra of EP on Pt(111) at four different coverages. EP was dosed onto the clean Pt(111) sample at 153 K, and the spectra were subsequently measured at 153 K. The coverages for spectra 1−4 correspond to 2.6, 1.2, 0.7, and 0.4 ML, respectively, as determined by XPS. The spectrum of clean Pt(111) is also provided for comparison. When a multilayer of EP was dosed at 153 K and the sample was heated to 213 K, a spectrum was obtained, which can be best described as intermediate between spectra 2 and 3 in Figure 5. This suggests that spectrum 2 (3) corresponds to a coverage slightly over (under) one monolayer and that EP does not undergo major chemical changes in the temperature range from 153 to 213 K.

At low coverage, the low-binding-energy spectrum is dominated by the intense platinum bands at 1.5 and 4.2 eV, which cover the comparably weak EP bands. On the other hand, the evolution of the deeper levels can be followed from multilayer to submonolayer coverage. As the coverage increases from monolayer to multilayer, all of the deeper levels shift by about 0.9 eV with respect to the Fermi level, as indicated by the dotted lines in Figure 5. At the same time, the intensity distribution within the broad band ranging from about 7 to 10 eV seems to change. The calculations indicate that this broad band comprises nine transitions (Figure 4). However, because the individual transitions are not resolved, it is not possible to draw conclusive information from this feature.

In contrast to this, the orbitals closest to the Fermi level are nicely separated and can be unambiguously identified as the lone-pair orbitals. The band at 4.1 eV in the multilayer spectrum associated with $n_{0(O1,O2)}$ shifts to 3.8 eV at 1.2 ML, whereas the band at 5.6 eV associated with $n_{0(O3)}$ and $n_0'_{(O1,O2)}$ shifts to 4.6 eV. Thus, the latter two orbitals show the same shift of about 0.9 eV as the deeper orbitals when going from multilayers to 1.2 ML. In contrast, $n_{0(O1,O2)}$ shifts by only 0.3 eV. This shows that the $n_{0(O1,O2)}$ lone-pair orbital is stabilized upon interaction with the Pt surface, thus indicating bonding of this orbital with empty d bands of Pt.

Figure 6 shows the same UP spectra as Figure 5 but with the spectrum of clean Pt(111) (Figure 5, trace 5) subtracted, such that the Pt band at 1.5 eV has vanished. In these difference spectra, the lone-pair orbitals of EP, which for the low-coverage spectra in Figure 5 were buried under the intense Pt band at 4.2 eV, can also be observed. When the coverage is increased from 0.4 to 0.7 and 1.2 ML, the lone-pair orbitals do not shift much, indicating the same bonding mechanism at low and high coverage. The stabilization of the $n_{0(O1,O2)}$ lone-pair orbital with respect to the other orbitals when going from multilayers to submonolayers amounts to about 0.7 eV.

4. Discussion

The large shift observed in the XP spectra of EP when going from multi- to monolayers can be due to relaxation effects (final-state effect) and chemical shifts due to bonding to the metal surface (initial-state effect). Likely both effects are involved. For physisorbed molecules within the multilayer the core ionized state relaxes because of interactions with the polarizable surroundings and the image potential. For chemisorbed molecules, metallic orbitals are involved in the bonding. The core ionized state can lose part of its ionic character because of

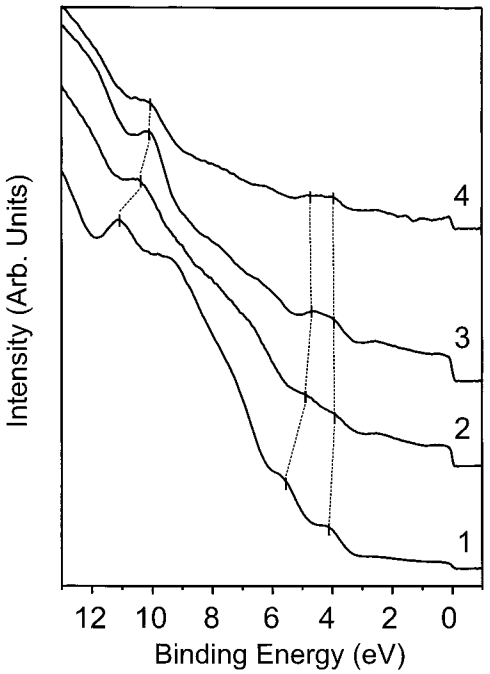

Figure 6. Same UP spectra of ethyl pyruvate on Pt(111) as in Figure 5 with the spectrum of clean Pt(111) subtracted such that the Pt band at 1.5 eV has vanished. The coverages, as determined by XPS, are (1) 2.6 ML (multilayers), (2) 1.2 ML, (3) 0.7 ML, and (4) 0.4 ML.

external screening from the metal, which shifts the ionization potential to lower energy.[19,20] The large observed shift in C and O 1s binding energies when going from multi- to monolayer (Figures 2 and 3) is thus an indication of a strong interaction between EP and the Pt surface. Similar shifts have been observed for propanoic acid, acrylic acid, and methyl methacrylate adsorbed on Pt(111), whereas for acrolein, which seems to interact only weakly with Pt(111), the binding energy shift between multi- and monolayer is marginal.[18] The observed change in the shape of the C1s XP spectra upon going from multi- to monolayer also shows that a strong chemisorption bond between EP and the Pt surface is formed. The observed shift of the C2 1s band further indicates that the ketone group is involved in the bonding to the surface. Additional insight into the nature of this interaction can be gained from the UP spectra.

A comparison of the EP multilayer and submonolayer UP spectra (Figures 5 and 6) reveals that the highest-occupied orbital $n_{O(O1,O2)}$ is stabilized by about 0.7 eV with respect to the other orbitals upon chemisorption. The involvement of this orbital in the bonding to the Pt surface necessarily results in an electron transfer from $n_{O(O1,O2)}$ to empty Pt d orbitals. Such a charge transfer to the metal is likely to be partially compensated by back-donation from metal bands into empty orbitals of EP. Probably the most popular example for such a bonding mechanism is CO adsorption on metal surfaces, the essence of which is described by the Blyholder model.[21] It consists of the interaction of the HOMO (5σ orbital) and LUMO ($2\pi^*$ orbital) frontier orbitals with metal d orbitals. Charge flows from the molecular 5σ orbital of CO to the metal d orbitals, which back-donate some charge into the molecular $2\pi^*$ orbital. This interaction manifests itself in a stabilization of the 5σ orbital by about 1 eV, as revealed by UPS.[22] A similar bonding mechanism was also proposed for acetone on Pt(111),[10] where an end-on (upright) mode was found. Our experimental findings indicate that the bonding mechanism for EP is analogous to that for CO and acetone, as described above. Specifically, the stabilization of the $n_{0(O1,O2)}$ lone-pair orbital of EP of 0.7 eV upon chemisorption is similar to the stabilization found for the 5σ lone-pair orbital of CO.[22] The interaction of $n_{O(O1,O2)}$ with empty d orbitals leads to a charge transfer toward the metal and a stabilization of the $n_{O(O1,O2)}$ orbital, as revealed by UPS. Likely the Pt metal back-donates some charge into low-lying empty EP orbitals, especially the π^* LUMO depicted in Figure 1, similar to what has been calculated for acetone.[8] This back-donation only marginally affects the UP spectra as it involves initially empty EP orbitals. However, the observed shift in the 1s binding energy of C2 can be interpreted along this line, as detailed in the following.

From a systematic comparison of XPS and NEXAFS spectra (in which the final state is a neutral, "self-screened" state) of CO on different metal surfaces it was concluded that relaxation must be considered as the major source of the observed changes in the XP spectra.[20] It was also shown that the XPS final state is sensitive to the chemical environment and, hence, the strength of the chemisorption bond, in contrast to the resonantly excited state observed in NEXAFS. The O1s peak corresponding to the well-screened final state shifts about 2 eV to lower binding energies when moving from weakly to strongly bound CO. Note that CO adsorbs via its C end. Still, the O atom strongly "feels" the adsorption as it contributes to the orbitals involved in the bonding to the surface. Similarly, in EP, C2 strongly feels back-donation into the LUMO (π^*_1) as C2 strongly contributes to this orbital. This, in turn, leads to enhanced screening of the C2 1s core hole in the XPS final state and, hence, a shift of the C2 1s band to lower binding energies in the XP spectrum, in a manner analogous to the observation made for the O1s in CO. In summary, our experimental findings for EP can be interpreted with a bonding mechanism very similar to the Blyholder model proposed for CO adsorption and found for acetone adsorption on Pt(111).

The bonding mechanism we observe for EP on Pt(111) is different from that found for other molecules with (conjugated) π systems, such as ethylene or benzene.[22,23] Ethylene and benzene chemisorption is dominated by charge transfer from the π orbital (HOMO) to the metal d orbitals and back-donation to the π^* orbital (LUMO), as described by Dewar, Chatt, and Duncanson.[24,25] From a molecular orbital point of view, two factors control the type and strength of bonding: (i) the overlap between metal and adsorbate orbitals and (ii) the fact that the energies of the interacting orbitals must be similar. The orbitals must have the same symmetry, and the spatial extent of the orbitals must be sufficient to allow overlap. d-metal surfaces offer a variety of orbitals, which can efficiently interact with adsorbate orbitals. In a perturbation theory picture,[26] the stabilization due to a bonding interaction between two orbitals is proportional to the inverse of their energy difference. Qualitatively, the different adorption behavior of ethylene and EP on Pt(111), i.e., π (di-σ) versus lone-pair bonding, can be understood from the energetics of the orbitals involved in the bonding to the metal surface. In ethylene, the HOMO is a π orbital, which donates electrons to the Pt metal orbitals. In EP, the π orbitals are stabilized because of the involvement of oxygen. This stabilization makes the energy difference between the π orbitals and the accepting metal orbitals near the Fermi level larger and, hence, this bonding mode less important. On the other hand, the lone-pair orbitals of EP are high in energy, which favors their bonding to the metal orbitals. Also important is the energy of the π^* orbital, which serves as an acceptor orbital in both bonding modes through the lone pair and through the π orbitals. Back-donation into this π^* orbital is more pronounced for the π-bonding mode, and hence, a low-lying

SCHEME 2: Qualitative Molecular Orbital Scheme for Ethyl Pyruvate and Ethylene[a]

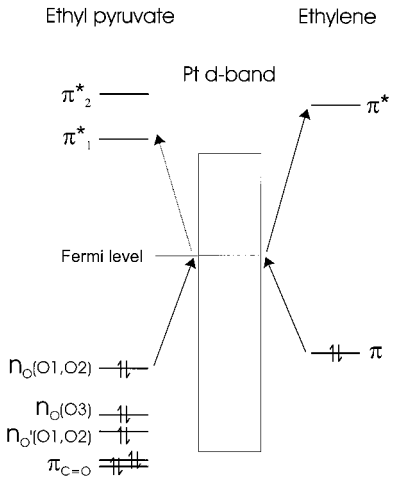

[a] Arrows indicate the major charge transfer upon binding to the platinum surface (ethyl pyruvate, lone-pair bonding; ethylene, di-σ bonding).

π* orbital favors this adsorption mode.[7] The above arguments are in line with comparative theoretical calculations for the adsorption of acetone (C═O group) and ethylene (C═C group) on Pt(111).[9] For ethylene, the di-σ adsorption mode with the C═C double bond parallel to the surface is calculated to be the most stable. For acetone, on the other hand, on-top adsorption with the C═O group in an upright position is predicted to be more stable than di-σ adsorption. The above molecular orbital discussion is qualitatively illustrated in Scheme 2, where the important molecular orbitals of EP and ethylene are given. The charge transfer upon bonding to the platinum surface is indicated by arrows.

The UPS and XPS data presented above do not give direct information about the orientation of EP with respect to the Pt(111) surface, i.e., whether EP is adsorbed in a parallel or perpendicular mode. In general, however, molecules adsorbed via lone-pair bonding tend to be in an upright position because of enhanced overlap between the lone pair and the metal orbitals in this arrangement. The nature of the lone pair itself directs the orientation of the molecule. In CO, for example, the lone pair (sp character) has only one lobe at the C atom bonded to the surface. Orbital overlap is maximized in a vertical orientation, which is consistent with the vertical orientation of adsorbed CO. In acetone, the lone pair has two lobes (sp^2 character) at the O atom bonding to the surface. Indeed, as has been demonstrated by electron energy loss spectroscopy, acetone is tilted in such a way that one lone-pair orbital lobe is directed to the surface, thus maximizing orbital overlap.[11] It is difficult to offer arguments concerning optimal orbital overlap for EP because the $n_{0(O1,O2)}$ lone pair (HOMO) is largely delocalized, as shown in Figure 1. It is conceivable that the bonding is via both O1 and O2, thus maximizing the orbital overlap through a two-center interaction with EP in its s-cis conformation. A mode similar to that found for acetone, in which only one orbital lobe is interacting and C2═O1 is tilted toward the surface (but the EP molecular plane is perpendicular to the surface), is also possible. In such an orientation, the repulsive four-electron interactions are minimal.[9] Finally, an arrangement is conceivable in which the EP molecular plane is tilted toward the surface, allowing additional orbital overlap with the "lobes" of $n_{0(O1,O2)}$ located between C1 and C2 and between C2 and C3. The observed shift in the C2 1s binding energy in the XPS upon chemisorption seems to indicate that the interaction is more strongly located at the ketone group (C2═O1).

Some additional information can be gained from the determined absolute coverage. In the saturated chemisorption layer, EP occupies around five Pt surface atoms. To appreciate this value, an estimate of the packing density has been calculated,[27] using a molecular unit cell ("box") for EP. An analogous procedure has been successfully applied to determine the orientation of adsorbed molecules from the measured coverage determined by Auger spectroscopy.[27] The EP unit cell was determined from the calculated gas-phase geometry taking into account the van der Waals radii,[27] resulting in a box of length 10.2 Å, width 6.0 Å, and height 4.2 Å for s-trans EP. This box occupies approximately nine, six, and four Pt atoms, depending on which side it is lying down. Similar results were obtained for the s-cis conformer. This estimate would indicate that EP in the saturated chemisorbed layer is not lying flat on the Pt surface (which would require approximately nine Pt surface atoms). For comparison, benzene on Pt(111), which is lying flat on Pt(111), occupies six to seven Pt surface atoms.[28] Hydroquinone, which has size similar to that of EP, occupies nine Pt surface atoms when adsorbed from solution onto Pt(111). Vibrational spectroscopy shows that it is adsorbed flat on the surface. At higher concentrations, a transition to vertically adsorbed hydroquinone is observed, which then occupies about five Pt surface atoms.[29]

From the initial change in work function (−0.73 eV at 0.1 ML absolute coverage) and the application of the Helmholtz equation,[30] a dipole moment perpendicular to the surface of 1.3 D per EP molecule can be derived. The work function change and, hence, the derived dipole moment have two origins. One is the net charge transfer between surface and adsorbate, and the other is the dipole moment of the adsorbate itself. The negative sign of the work function change is consistent with a net charge transfer from ethyl pyruvate to the Pt surface, hence decreasing the surface dipole moment, as expected for a lone-pair bonding mechanism. The magnitude of this initial change is, however, rather large, indicating that the dipole moment of ethyl pyruvate itself also contributes to the observed large initial change in work function. This again indicates that ethyl pyruvate is adsorbed in a tilted orientation, with the negatively charged end pointing toward the surface, rather than a completely flat orientation, as only the dipole moment component perpendicular to the surface affects the work function.

5. Conclusions

The findings presented in this work can be summarized as follows: (i) Ethyl pyruvate has largely delocalized molecular orbitals. (ii) Upon chemisorption of ethyl pyruvate onto Pt(111) at low temperatures, the HOMO lone-pair orbital is stabilized by about 0.7 eV with respect to the other orbitals. This shows that ethyl pyruvate is lone-pair-bonded to the Pt surface under these conditions. (iii) Lone-pair bonding is observed in the fully saturated chemisorption layer as well as far below saturation. (iv) The differences in the XP spectra of condensed and chemisorbed ethyl pyruvate indicate that the bonding is mainly localized at the ketone C═O group. (v) Calculated correlated ionization potentials are in good agreement with the measured UP spectra of ethyl pyruvate. (vi) The measured absolute coverage within the saturated chemisorption layer and the initial work function change upon adsorption indicate that ethyl pyruvate is predominantly adsorbed in a tilted rather than a completely flat mode.

The present findings concerning the adsorption mode of EP under low-temperature UHV conditions seem to challenge the

assumptions made in proposed mechanisms for the enantioselective hydrogenation of ethyl pyruvate over cinchonidine-modified platinum. Clearly, this work indicates that there are at least two important adsorption modes that must be distinguished, namely, lone-pair bound EP, as evidenced in the present low-temperature UHV work, and π- (or di-σ-) bonded EP, as postulated on the basis of catalytic experiments. The population density of species bound via these adsorption modes is expected to depend on various factors, such as surface coverage, temperature, and the presence of coadsorbed species. In this light, the present findings do not permit a final assessment of the adsorption mode of EP under reaction conditions of enantioselective hydrogenation. A final answer requires investigation of EP adsorption when coadsorbed with hydrogen, modifier, and solvent, which will be targeted in future work.

Note Added in Proof. After submission of this manuscript Castonguay and coworkers (Castonguay, M.; Roy, J.-R.; Rochefort, A.; McBreen, P. H. *J. Am. Chem. Soc.* **2000**, *122*, 518) published a vibrational spectroscopy study of methyl pyruvate on Ni(111), in which they show that the methyl pyruvate is predominantly adsorbed in s-cis conformation via the O lone pair, in full agreement with our findings for Pt(111).

References and Notes

(1) Baiker, A.; Blaser, H. U. Enantioselective Catalysts and Reactions. In *Handbook of Heterogeneous Catalysis*; Ertl, G., Knözinger, H., Weitkamp, J., Eds.; VCH Publishers: Weinheim, Germany, 1997; Vol. 5, p 2422.

(2) Izumi, Y. *Adv. Catal.* **1983**, *32*, 215.

(3) Orito, Y.; Imai, S.; Niwa, S. *J. Chem. Soc. Jpn.* **1979**, 1118.

(4) Simons, K. E.; Meheux, P. A.; Griffiths, S. P.; Sutherland, I. M.; Johnston, P.; Wells, P. B.; Carley, A. F.; Rajumon, M. K.; Roberts, M. W.; Ibbotson, A. *Recl. Trav. Chim. Pays-Bas* **1994**, *113*, 465.

(5) Schwalm, O.; Minder, B.; Weber, J.; Baiker, A. *Catal. Lett.* **1994**, *23*, 271.

(6) Baiker, A. *J. Mol. Catal. A: Chem.* **1997**, *115*, 473.

(7) Delbecq, F.; Sautet, P. *Langmuir* **1993**, *9*, 197.

(8) Delbecq, F.; Sautet, P. *Surf. Sci.* **1993**, *295*, 353.

(9) Delbecq, F.; Sautet, P. *J. Catal.* **1995**, *152*, 217.

(10) Avery, N. R.; Weinberg, W. H.; Anton, A. B.; Toby, B. H. *Phys. Rev. Lett.* **1983**, *51*, 682.

(11) Anton, A. B.; Avery, N. R.; Toby, B. H.; Weinberg, W. H. *J. Am. Chem. Soc.* **1986**, *108*, 684.

(12) Björneholm, O.; Nilsson, A.; Tillborg, H.; Bennich, P.; Sandall, A.; Hernnäs, B.; Puglia, C.; Martensson, N. *Surf. Sci.* **1994**, *315*, L983.

(13) Frisch, M. J.; Trucks, G. W.; Schlegel, H. B.; Gill, P. M. W.; Johnson, B. G.; Robb, M. A.; Cheeseman, J. R.; Keith, T.; Petersson, G. A.; Montgomery, J. A.; Raghavachari, K.; Al-Laham, M. A.; Zakrzewski, V. G.; Ortiz, J. V.; Foresman, J. B.; Cioslowski, J.; Stefanov, B. B.; Nanayakkara, A.; Challacombe, M.; Peng, C. Y.; Ayala, P. Y.; Chen, W.; Wong, M. W.; Andres, J. L.; Replogle, E. S.; Gomperts, R.; Martin, R. L.; Fox, D. J.; Binkley, J. S.; Defrees, D. J.; Baker, J.; Stewart, J. P.; Head-Gordon, M.; Gonzalez, C.; Pople., J. A. *Gaussian 94*, revision E.1; Gaussian Inc.: Pittsburgh, PA, 1995.

(14) Stewart, J. J. P. *J. Comput. Chem.* **1989**, 209.

(15) Cederbaum, L. S. *J. Phys. B: Atom. Mol. Phys.* **1975**, *8*, 290.

(16) Ferri, D.; Bürgi, T.; Baiker, A. *J. Chem. Soc., Perkin Trans. 2* **2000**, 221.

(17) Siegbahn, K.; Nordling, C.; Johansson, G.; Hedman, J.; Heden, P. F.; Hamrin, K.; Gelius, U.; Bergmark, T.; Werme, L. O.; Manne, R.; Baer, Y. *ESCA Applied to Free Molecules*; North-Holland Publishing Company: Amsterdam, 1969.

(18) Bournel, F.; Laffon, C.; Parent, P.; Tourillon, G. *Surf. Sci.* **1996**, *350*, 60.

(19) Ranke, W. *Surf. Sci.* **1989**, *209*, 57.

(20) Wurth, W.; Coulman, A.; Puschmann, A.; Menzel, D. *Phys. Rev. B* **1990**, *41*, 12933.

(21) Blyholder, G. *J. Phys. Chem.* **1964**, *68*, 2772.

(22) Brundle, C. R. Spectroscopy of Metal Surfaces and Adsorbed Species. In *Electronic Structure and Reactivity of Metal Surfaces*; Derouane, E. G., Lucas, A. A., Eds.; Plenum Press: New York, 1976; p 389.

(23) Demuth, J. E.; Eastman, D. E. *Phys. Rev. Lett.* **1974**, *32*, 1123.

(24) Dewar, M. J. S. *Bull. Soc. Chim. Fr.* **1951**, *18*, C79.

(25) Chatt, J.; Duncanson, L. A. *J. Chem. Soc.* **1953**, 2939.

(26) Atkins, P. W. *Molecular Quantum Mechanics*; Oxford University Press: Oxford, U.K., 1983.

(27) Hubbard, A. T. *Chem. Rev.* **1988**, *88*, 633.

(28) Yau, S. L.; Kim, Y. G.; Itaya, K. *J. Am. Chem. Soc.* **1996**, *118*, 7795.

(29) Lu, F.; Salaita, G. N.; Laguren-Davidson, L.; Stern, D. A.; Wellner, E.; Frank, D. G.; Batina, N.; Zapien, D. C.; Walton, N.; Hubbard, A. T. *Langmuir* **1988**, *4*, 637.

(30) Somorjai, G. A. *Introduction to Surface Chemistry and Catalysis*; John Wiley: New York, 1994.